

Variants of thick-restart Lanczos for the Bethe–Salpeter eigenvalue problem*

Fernando Alvarruiz[†]

Blanca Mellado-Pinto[‡]

Jose E. Roman[§]

March 28, 2025

Abstract

The non-Hermitian Bethe–Salpeter eigenvalue problem is a structured eigenproblem, with real eigenvalues coming in pairs $\{\lambda, -\lambda\}$ where the corresponding pair of eigenvectors are closely related, and furthermore the left eigenvectors can be trivially obtained from the right ones. We exploit these properties to devise three variants of structure-preserving Lanczos eigensolvers to compute a subset of eigenvalues (those of either smallest or largest magnitude) together with their corresponding right and left eigenvectors. For this to be effective in real applications, we need to incorporate a thick-restart technique in a way that the overall computation preserves the problem structure. The new methods are validated in an implementation within the SLEPc library using several test matrices, some of them coming from the Yambo materials science code.

1 Introduction

We are concerned with the eigenvalue problem $Hx = \lambda x$, where the matrix has the form

$$H = \begin{bmatrix} R & C \\ -C^* & -R^T \end{bmatrix} \in \mathbb{C}^{2n \times 2n}, \quad (1)$$

with $R, C \in \mathbb{C}^{n \times n}$ and $R = R^*$, $C = C^T$. We use the \cdot^T and \cdot^* superscripts to denote transposition and complex conjugate transposition, respectively. In addition to eigenvalues λ and right eigenvectors x , we are also interested in computing left eigenvectors y , i.e., those vectors satisfying the relation $y^*H = \bar{\lambda}y^*$. Furthermore, when a certain condition is met, to be discussed later on, all eigenvalues are real so we have $y^*H = \lambda y^*$.

Matrix H in (1) is called the Bethe–Salpeter Hamiltonian matrix as it stems from the Bethe–Salpeter equation [28]. This equation is relevant in the analysis of optical absorption and emission processes in solid-state systems by means of first-principles calculation based on

*This work was supported by grants PID2022-139568NB-I00 and RED2022-134176-T funded by MCIN/AEI/10.13039/501100011033 and by “ERDF A way of making Europe”. Innovation Study ISOLV-BSE has received funding through the Inno4scale project, which is funded by the European High-Performance Computing Joint Undertaking (JU) under Grant Agreement No 101118139. The JU receives support from the European Union’s Horizon Europe Programme. The second author was also supported by Universitat Politècnica de València in its PAID-01-23 program.

[†]D. Sistemes Informàtics i Computació, Universitat Politècnica de València, València, Spain (fbermejo@dsic.upv.es).

[‡]D. Sistemes Informàtics i Computació, Universitat Politècnica de València, València, Spain (bmelpin@dsic.upv.es).

[§]D. Sistemes Informàtics i Computació, Universitat Politècnica de València, València, Spain (jroman@dsic.upv.es).

Green’s function theory. This is one of the main functionalities offered by the Yambo simulation code [23, 2, 29]. Starting from a Density Functional Theory (DFT) approximation, Yambo is able to perform additional computations to formulate a Bethe–Salpeter eigenproblem from which to obtain excited-state properties such as energies of quasiparticles. An example of quasiparticle is the so called *exciton*, consisting of a bound state of an electron and a hole; understanding the behaviour of excitons gives valuable information about optical properties of new materials such as two-dimensional extended structures. Other simulation codes with similar goals are BerkeleyGW [13], MOLGW [9], and VOTCA-XTP [35]. Some of these codes are restricted to a particular case of the BSE problem called the linear response eigenvalue problem, as will be discussed in section 2.1. With these tools, it is possible to predict the optical behavior of materials, which is important to design more efficient photovoltaic and light-emitting devices, and in many other applications.

The diagonal blocks of H are associated with the resonant (R) and anti-resonant transitions, i.e., from occupied to empty states and from empty to occupied, respectively. In the general case, the anti-resonant terms may be unrelated to R , but in most types of analyses both blocks have a certain mutual symmetry relation, and this is what confers special algebraic properties on H . The off-diagonal block (C) is related to coupling between the two types of transitions. If coupling is small, then these terms can be neglected and the problem can be simplified to a Hermitian eigenproblem for R (the so called Tamm-Dancoff approximation). However, in many interesting applications keeping the coupling is of key importance and hence the problem must be formulated as in (1).

For most physical systems, H is a *definite* Bethe–Salpeter Hamiltonian matrix. This will be defined formally in the next section, but it essentially means that if we remove the minus signs in the bottom block-row, the resulting matrix is Hermitian and positive definite. We will assume this property throughout the paper. In that case, all eigenvalues λ are real, as will be shown with more detail later on.

The Bethe–Salpeter equation belongs to a specific class of structured eigenvalue problems. Structured eigenproblems [21, 14] are those whose defining matrices are structured, i.e., their N^2 entries depend on less than N^2 parameters (with $N = 2n$ in our case). Apart from the most obvious Hermitian class, we can find many other classes of structured matrices such as skew-Hermitian, Hamiltonian, unitary, and symplectic, to name a few [10]. Preserving the structure can help preserve physically relevant symmetries in the eigenvalues of the matrix and may improve the accuracy and efficiency of the eigensolver. For example, in quadratic eigenvalue problems arising from gyroscopic systems, eigenvalues appear in quadruples $\{\lambda, -\lambda, \bar{\lambda}, -\bar{\lambda}\}$, i.e., the spectrum is symmetric with respect to both the real and imaginary axes. This problem can be linearized to a 2×2 -block Hamiltonian/skew-Hamiltonian matrix pencil with the same eigenvalues. A structure-preserving eigensolver will give a more accurate answer because it enforces the structure throughout the computation. We can find in the literature many proposals to adapt both direct and iterative methods to particular classes of structured eigenproblems. For instance, in the last decades Krylov methods for Hamiltonian and related eigenproblems have been developed [24, 36, 5, 6].

Matrix H belongs to the class of complex J -symmetric matrices [10, 7], where $J = \begin{bmatrix} 0 & I \\ -I & 0 \end{bmatrix}$. But the definite Bethe–Salpeter matrices exhibit even more structure, leading to properties such that eigenvalues are real and come in pairs $\{\lambda, -\lambda\}$, with a close relation between eigenvectors associated to the positive and negative eigenvalues, as well as with their corresponding left eigenvectors. All this will be presented in detail in section 2.

Several authors have recently addressed the Bethe–Salpeter eigenvalue problem from the perspective of structure-preserving eigensolvers. Penke and co-authors [27, 26] have devised effective dense eigensolvers to compute the full eigendecomposition of H . On the other hand, Shao

and co-authors also focused initially on the computation of the full eigenspectrum with direct methods [31], but then turned their attention to iterative methods [30], which are able to approximate the optical absorption spectrum without having to compute all eigenvalues. This latter work builds upon previous contributions from the computational physics community [15, 16], providing a more formal view in terms of numerical analysis. The article of Shao *et al.* [30] is also the starting point of our work, and has been our inspiration to develop the three methods proposed in section 3. The key difference between our work and the cited papers is that we are interested in using Lanczos-type methods to explicitly compute a subset of eigenvalues with the corresponding (right and left) eigenvectors, whereas the previous works employ Lanczos recurrences combined with quadrature rules to evaluate the matrix function that is mathematically related to the definition of the optical absorption spectrum. In our case, the eigenvalues and eigenvectors can then be used to reconstruct the optical spectrum, but in addition they provide more information about the spatial distribution of the wave function associated with each excited energy.

Our main contribution is the addition of restart techniques to the Lanczos methods for Bethe–Salpeter. The Lanczos algorithms of Shao *et al.* [30] and Grüning *et al.* [15] rely on a plain Lanczos recurrence. It is well-known that this simple recurrence suffers from loss of orthogonality among the Lanczos vectors, resulting in spurious duplicates of approximate eigenvalues. This phenomenon is benign in the case of approximating the optical absorption spectrum directly. In contrast, when we want to compute eigentriplets accurately, it is necessary to avoid the loss of orthogonality by some kind of reorthogonalization. As a consequence, it is compulsory to keep all the previously computed Lanczos vectors, which increases memory cost in a practical implementation. Restarting techniques aim at alleviating this problem, by bounding the maximum number of vectors to be kept. The thick-restart Lanczos method [37] is a very effective restart technique that is able to compress the basis of Lanczos vectors while preserving the most relevant spectral information generated so far. It is a particular instance of the more general Krylov–Schur method for non-Hermitian matrices [33].

Our goal is to adapt the thick-restart Lanczos technique to the Bethe–Salpeter eigenproblem, as we have done before in other classes of problems such as the SVD [18] or the GSVD [1]. The challenge in the case of Bethe–Salpeter is that the restarting step, in addition to preserving the wanted eigenvalues in the compressed basis, must do so in a way that it keeps the problem structure, so that the full computation is still structure-preserving. We will show how to do this in three flavours of Lanczos methods, in section 3.

We have implemented our methods in SLEPc, the Scalable Library for Eigenvalue Problem Computations [19]. Section 4 discusses some implementation details. SLEPc is freely available and widely used in many scientific computing projects around the world. In particular, the Yambo code has the capability to solve the Bethe–Salpeter equation via SLEPc. The development of the new solvers has been done in close collaboration with the Yambo developers. Yambo users will seamlessly benefit from the new solvers’ improved accuracy and increased efficiency, being able to pursue more challenging investigations. As examples of promising materials analyzed by Yambo users with the help of SLEPc, we can mention bismuth triiodide [12], black phosphorus [34], and metallic MXene multilayers [20]. In section 5 we illustrate the performance of the new solvers with several test cases, some of them coming from real analyses using Yambo.

2 Problem definition

In this section we provide more details about the Bethe–Salpeter matrix and its properties, and review previous efforts to apply Lanczos methods to it in a structure-preserving way.

2.1 The Bethe–Salpeter eigenproblem

Since R is Hermitian and C is complex symmetric, matrix H in (1) can also be expressed as

$$H = \begin{bmatrix} R & C \\ -\overline{C} & -\overline{R} \end{bmatrix}, \quad (2)$$

where the bar indicates complex conjugation. In some applications, e.g., systems with real-space inversion symmetry, R and C are real and hence the Bethe–Salpeter matrix is also real, $H = \begin{bmatrix} R & C \\ -C & -R \end{bmatrix}$. Shao and coauthors [30] propose a specific method for this case. This is called the linear response eigenvalue problem (LREP) and has been studied in a series of papers by Bai and Li [3, 4]. Benner and Penke [8] also analyze the linear response eigenvalue problem, but with complex R and C . In our case, we consider only the form (1) with complex matrices, but we remark that the methods proposed in section 3 can be applied to real matrices without any change.

To derive the algorithms, it will be helpful to factor out the signs in H ,

$$H = S\hat{H}, \quad S = \begin{bmatrix} I & 0 \\ 0 & -I \end{bmatrix}, \quad \hat{H} = \begin{bmatrix} R & C \\ \overline{C} & \overline{R} \end{bmatrix}, \quad (3)$$

where I denotes the $n \times n$ identity matrix, S is a signature matrix and \hat{H} is Hermitian. As mentioned in section 1, we are interested in the case when \hat{H} is positive definite, in which case we say H is a definite Bethe–Salpeter matrix. Throughout the paper, we will assume that this property holds, which is generally true in most applications.

The Bethe–Salpeter matrix H belongs to the slightly more general class of complex J -symmetric matrices, that can be written as

$$H_C = \begin{bmatrix} R & C \\ D & -R^T \end{bmatrix} \in \mathbb{C}^{2n \times 2n}, \quad R, C = C^T, D = D^T \in \mathbb{C}^{n \times n}. \quad (4)$$

These matrices satisfy $JH_C = (JH_C)^T$, where $J = \begin{bmatrix} 0 & I \\ -I & 0 \end{bmatrix}$. The eigenvalues of complex J -symmetric matrices display a symmetry [10, 7]: they appear in pairs $\{\lambda, -\lambda\}$. Also, if x is the right eigenvector for λ , $H_C x = \lambda x$, then $J\bar{x}$ is the left eigenvector for $-\lambda$,

$$(J\bar{x})^* H_C = -\lambda (J\bar{x})^*. \quad (5)$$

The Bethe–Salpeter matrix H inherits these properties, but has some additional structure. Since H is the product of two Hermitian matrices, one of them positive definite, (3), then it is diagonalizable and has real spectrum. Due to this fact, a specific version of the property in (5) can be proved [31]:

Theorem 1 (Shao *et al.* [31]). *Let H be of the form (1) satisfying that \hat{H} in (3) is positive definite. Then there exist $X_1, X_2 \in \mathbb{C}^{n \times n}$ and positive numbers $\lambda_1, \lambda_2, \dots, \lambda_n \in \mathbb{R}$ such that*

$$HX = X \begin{bmatrix} \Lambda_+ & 0 \\ 0 & -\Lambda_+ \end{bmatrix}, \quad Y^* H = \begin{bmatrix} \Lambda_+ & 0 \\ 0 & -\Lambda_+ \end{bmatrix} Y^*, \quad Y^* X = I_{2n}, \quad (6)$$

where

$$X = \begin{bmatrix} X_1 & \overline{X_2} \\ X_2 & \overline{X_1} \end{bmatrix}, \quad Y = \begin{bmatrix} X_1 & -\overline{X_2} \\ -X_2 & \overline{X_1} \end{bmatrix}, \quad (7)$$

and $\Lambda_+ = \text{diag}\{\lambda_1, \dots, \lambda_n\}$.

The previous theorem provides a complete description of the eigendecomposition of H , showing that there is considerable redundancy. Efficient eigensolvers should exploit this fact to compute the solution faster.

For large-scale problems, computing the full eigendecomposition is too costly. For an accurate enough approximation of the optical absorption spectrum, it is sufficient to compute a few eigenvalues and their corresponding eigenvectors. That is why we focus on iterative eigensolvers, particularly Lanczos methods that can provide good approximations to exterior eigenvalues in relatively few iterations. Here we remark that matrices coming from Green’s function theory such as those in the Yambo code are dense, while Lanczos is most appropriate in the case of sparse matrices, or more generally when matrix-vector products are cheap. Still, this approach can be competitive with respect to full diagonalization, provided that the number of wanted eigenvalues is not too large. In this paper, we assume that the user is interested in a few hundreds of eigenvalues at most.

The eigenvalues of interest in applications are those of smallest magnitude, i.e., the smallest energies. Due to the $\{\lambda, -\lambda\}$ symmetry, those eigenvalues lie in the middle of the spectrum, which is a bad scenario for the convergence of Lanczos methods. However, the variants of Lanczos presented in section 3 work around this issue by some kind of *spectrum folding* approach, where negative eigenvalues become positive. Essentially, the proposed methods compute only $\lambda \in \Lambda_+$ with corresponding eigenvectors, and then use theorem 1 to inexpensively reconstruct the spectral elements for $-\lambda$, including left eigenvectors which are also required by the application. Hence, techniques such as the shift-and-invert spectral transformation for computing interior eigenvalues are not usually necessary, unless eigenvalues are clustered together close to zero. Still, in section 4 we discuss how this technique can be implemented in our Bethe–Salpeter solvers.

2.2 Possible solution approaches and related work

The most naive solution approach is to use a general non-Hermitian Krylov solver, configuring it to search for smallest magnitude eigenvalues. It must be capable of computing left eigenvectors as well. For this, SLEPc provides an implementation of two-sided Krylov–Schur [39]. This was the strategy used by the Yambo code prior to the work presented in this paper. A better approach would be to use plain Krylov–Schur to obtain right eigenvectors only, and then apply theorem 1 to obtain left eigenvectors. Still, this method is not recommended because it is not structure-preserving. This latter approach will be the baseline for the performance comparisons in section 5.

The Bethe–Salpeter eigenvalue problem can be converted to a real Hamiltonian eigenvalue problem [31, Thm. 2], and this connection has been exploited by some authors to develop full diagonalization eigensolvers [31, 27]. Similarly, we could adapt the structure-preserving Krylov methods for Hamiltonian eigenvalue problems mentioned in section 1. However, this would exploit only part of the structure, and disregard the richer structure given by theorem 1. Although we do not consider this route here, we remark that it would be a potentially good approach in case of non-definite problems, i.e., when \hat{H} is not definite, in which case the methods of section 3 cannot be applied.

In view of (3), we could consider a methodology for the product eigenvalue problem. The details for periodic Krylov–Schur have been worked out by Kressner [22]. If we applied this method to (3), we would obtain a periodic Krylov decomposition with two blocks, where the projected problem would contain an upper Hessenberg and an upper triangular block, to which it is possible to apply a Krylov–Schur-type restart. Interestingly, the Lanczos decompositions that we will describe in detail in section 3 resemble this, but with tridiagonal and diagonal blocks since we additionally exploit the symmetries underlying the problem structure.

To understand these symmetries, we have to interpret (3) as a generalized eigenvalue problem. If we consider the pencil (S, \hat{H}) , we have a Hermitian definite generalized eigenproblem where we can apply a B -Lanczos recurrence with the inner product induced by \hat{H} . The Bethe–Salpeter matrix H is self-adjoint with respect to this inner product, and Lanczos will produce a real symmetric tridiagonal matrix containing Ritz approximations of the eigenvalues of H . An alternative would be to consider the matrix pair (\hat{H}, S) . It can be shown that H is also self-adjoint with respect to the indefinite inner product induced by S , so an analogous approach could be applied using a pseudo-Lanczos recurrence. We note that SLEPc provides an implementation of pseudo-Lanczos that can be useful in some settings [11], but it is better to avoid it since numerical stability cannot be guaranteed. The approach with definite inner product is to be preferred, even though inner products for \hat{H} are much more expensive than those for S . The good news is that the methods presented below get around the high cost of \hat{H} -inner products and never need to compute them explicitly.

Shao and coauthors [30] propose a structure-preserving Lanczos process using \hat{H} -inner products. There is a connection between the quantities computed by this method and a Lanczos decomposition for H^2 . This implicit squaring of the matrix has the effect of folding the spectrum around zero so that all eigenvalues become positive. This method is described in detail in section 3.1. The last part of [30] analyzes the connection of their method with other Lanczos methods. One of them is due to Grüning *et al.* [15] and we will discuss it in section 3.2. Another variation is also analyzed in connection with symplectic Lanczos, where the projected eigenproblem of the Lanczos factorization has again a Bethe–Salpeter structure, see the details in section 3.3. As mentioned in section 1, all these methods were originally intended for computing the absorption spectrum directly via quadrature rules. In contrast, our presentation of the methods in section 3 focuses on computation of eigenvalues and eigenvectors, with an effective restart.

We conclude this section by mentioning an additional strategy for solving the Bethe–Salpeter eigenproblem. It is possible to build an equivalent product eigenvalue problem defined by two real matrices of order $2n$ [38]. A similar product eigenvalue problem is often used as a proxy for solving the LREP, so this opens the door to using, in the context of the Bethe–Salpeter eigenproblem, methods that have been successfully employed in the LREP, such as several variants of LOBPCG [38].

3 Thick restart Lanczos

The three methods discussed in this section are mathematically equivalent, since they are based on equivalent Lanczos recurrences, only differing in the way the different quantities are computed. Computational results in section 5 will show that all of them provide good accuracy and performance.

Throughout this section we will use the following notation. The $k \times k$ identity matrix is denoted by I_k and the j th column of the identity is denoted by e_j , where the length of the vector is implicitly defined by the context. For matrices representing basis vectors such as V_k , the subindex denotes the number of columns, while in square matrices such as the tridiagonal T_k , the subindex refers to dimension in both rows and columns. The non-standard inner product induced by a Hermitian positive-definite matrix B is denoted by $(x, y)_B = y^* B x$, and similarly the corresponding norm is $\|x\|_B = \sqrt{x^* B x}$. The imaginary unit will be denoted by i (in roman) and $\text{Re}(\cdot)$ and $\text{Im}(\cdot)$ will respectively denote the real and imaginary parts of a complex entity.

3.1 Method based on Shao *et al*

3.1.1 Lanczos recurrence

The Lanczos procedure proposed in [30] builds the Lanczos-type relation

$$H \begin{bmatrix} U_k & V_k \\ \bar{U}_k & -\bar{V}_k \end{bmatrix} = \begin{bmatrix} U_k & V_k \\ \bar{U}_k & -\bar{V}_k \end{bmatrix} \begin{bmatrix} 0 & T_k \\ I_k & 0 \end{bmatrix} + \beta_k \begin{bmatrix} u_{k+1} \\ \bar{u}_{k+1} \end{bmatrix} e_{2k}^*, \quad (8)$$

where $U_k, V_k \in \mathbb{C}^{n \times k}$, $U_k = [u_1, \dots, u_k]$, $V_k = [v_1, \dots, v_k]$, and T_k is the real symmetric tridiagonal positive definite matrix

$$T_k = \text{tridiag} \begin{Bmatrix} \beta_1 & \cdots & \beta_{k-1} \\ \alpha_1 & \cdots & \alpha_k \\ \beta_1 & \cdots & \beta_{k-1} \end{Bmatrix}.$$

Lanczos vectors satisfy the orthogonality condition

$$\begin{bmatrix} V_k & U_k \\ \bar{V}_k & -\bar{U}_k \end{bmatrix}^* \begin{bmatrix} U_k & V_k \\ \bar{U}_k & -\bar{V}_k \end{bmatrix} = 2I_{2k}. \quad (9)$$

Assuming $u_{j-1}, u_j, v_j, \beta_{j-1}$, are available for a given $j \geq 1$, with $u_0 = 0$, new vectors are computed by first generating

$$\begin{aligned} \tilde{u}_{j+1} &= Rv_j - C\bar{v}_j - \beta_{j-1}u_{j-1} - \alpha_j u_j, \\ \tilde{v}_{j+1} &= R\tilde{u}_{j+1} + C\bar{\tilde{u}}_{j+1}, \end{aligned}$$

where $\alpha_j = \text{Re}(v_j^*(Rv_j - C\bar{v}_j))$, and then normalizing to obtain

$$u_{j+1} = \tilde{u}_{j+1}/\beta_j, \quad v_{j+1} = \tilde{v}_{j+1}/\beta_j, \quad \text{with } \beta_j = \sqrt{\text{Re}(\tilde{u}_{j+1}^* \tilde{v}_{j+1})}.$$

Initial vectors can be generated from an arbitrary \tilde{u}_1 , by computing $\tilde{v}_1 = R\tilde{u}_1 + C\bar{\tilde{u}}_1$ and normalizing

$$u_1 = \tilde{u}_1/\beta_0, \quad v_1 = \tilde{v}_1/\beta_0, \quad \text{with } \beta_0 = \sqrt{\text{Re}(\tilde{u}_1^* \tilde{v}_1)}.$$

As shown in [30], matrices U_k and T_k can equivalently be obtained by applying a k -step Lanczos procedure to H^2 with the \hat{H} -inner product, resulting in

$$H^2 \begin{bmatrix} U_k \\ \bar{U}_k \end{bmatrix} = \begin{bmatrix} U_k \\ \bar{U}_k \end{bmatrix} T_k + \beta_k \begin{bmatrix} u_{k+1} \\ \bar{u}_{k+1} \end{bmatrix} e_k^*,$$

with the orthogonality condition corresponding to (9) being

$$\begin{bmatrix} U_k \\ \bar{U}_k \end{bmatrix}^* \hat{H} \begin{bmatrix} U_k \\ \bar{U}_k \end{bmatrix} = 2I_k.$$

3.1.2 Reorthogonalization

As mentioned in section 1, loss of orthogonality in the Lanczos recurrence to build (8) is not a problem when using it to compute the absorption spectrum, as in [30], but must be avoided in our case, because our goal is to compute the eigenvalues and eigenvectors. Our approach is to do full reorthogonalization at each Lanczos step, see section 4 for additional discussion. We show next how to implement reorthogonalization in Shao's method.

Suppose orthogonality of vector \tilde{u}_{j+1} is not perfect, so that we have

$$\beta_j \begin{bmatrix} u_{j+1} \\ \bar{u}_{j+1} \end{bmatrix} = \begin{bmatrix} \tilde{u}_{j+1} \\ \tilde{\bar{u}}_{j+1} \end{bmatrix} - \begin{bmatrix} U_j & V_j \\ \bar{U}_j & -\bar{V}_j \end{bmatrix} \begin{bmatrix} c \\ d \end{bmatrix},$$

with c, d not zero. Premultiplying by $\begin{bmatrix} V_j & U_j \\ \bar{V}_j & -\bar{U}_j \end{bmatrix}^*$ and taking into account the orthogonality condition (9), we get

$$\begin{bmatrix} c \\ d \end{bmatrix} = \frac{1}{2} \begin{bmatrix} V_j & U_j \\ \bar{V}_j & -\bar{U}_j \end{bmatrix}^* \begin{bmatrix} \tilde{u}_{j+1} \\ \tilde{\bar{u}}_{j+1} \end{bmatrix},$$

which leads to

$$\begin{aligned} c &= \text{Re}(V_j^* \tilde{u}_{j+1}), \\ d &= \text{Im}(U_j^* \tilde{u}_{j+1})i. \end{aligned}$$

After computing c, d , a reorthogonalized vector \check{u}_{j+1} is obtained as

$$\check{u}_{j+1} = \beta_j u_{j+1} = \tilde{u}_{j+1} - U_j c - V_j d.$$

The resulting Lanczos process is described by means of algorithm 1.

ALGORITHM 1: Shao's Lanczos with reorthogonalization

Input: A definite $2n \times 2n$ BSE matrix H with structure (1); initial vector \tilde{u}_1 of size n ; number of Lanczos steps k .

Output: U_k, V_k, T_k making up Lanczos-type decomposition (8).

```

1:  $\tilde{v}_1 = R\tilde{u}_1 + C\tilde{\bar{u}}_1$ 
2:  $\beta_0 = \sqrt{\text{Re}(\tilde{u}_1^* \tilde{v}_1)}$ ,  $u_0 = 0$ 
3:  $u_1 = \tilde{u}_1/\beta_0$ ,  $v_1 = \tilde{v}_1/\beta_0$ 
4: for  $j = 1, 2, \dots, k$  do
5:    $x = Rv_j - C\bar{v}_j$ 
6:    $\tilde{\alpha}_j = \text{Re}(v_j^* x)$ 
7:    $\tilde{u}_{j+1} = x - \beta_{j-1}u_{j-1} - \tilde{\alpha}_j u_j$ 
8:    $c = \text{Re}(V_j^* \tilde{u}_{j+1})$ ,  $d = \text{Im}(U_j^* \tilde{u}_{j+1})i$ 
9:    $\alpha_j = \tilde{\alpha}_j + c_j$ 
10:   $\check{u}_{j+1} = \tilde{u}_{j+1} - U_j c - V_j d$ 
11:   $\check{v}_{j+1} = R\check{u}_{j+1} + C\check{\bar{u}}_{j+1}$ 
12:   $\beta_j = \sqrt{\text{Re}(\check{u}_{j+1}^* \check{v}_{j+1})}$ 
13:   $u_{j+1} = \check{u}_{j+1}/\beta_j$ ,  $v_{j+1} = \check{v}_{j+1}/\beta_j$ 
14: end for
```

3.1.3 Restart

Let $T_k = QD_kQ^*$, with Q orthogonal, be the eigendecomposition of T_k . Then,

$$\begin{bmatrix} 0 & T_k \\ I_k & 0 \end{bmatrix} = \begin{bmatrix} Q & 0 \\ 0 & Q \end{bmatrix} \begin{bmatrix} 0 & D_k \\ I_k & 0 \end{bmatrix} \begin{bmatrix} Q^* & 0 \\ 0 & Q^* \end{bmatrix}.$$

Substituting in (8) and multiplying on the right by $\begin{bmatrix} Q & 0 \\ 0 & Q \end{bmatrix}$, we get

$$H \begin{bmatrix} U_k Q & V_k Q \\ \bar{U}_k Q & -\bar{V}_k Q \end{bmatrix} = \begin{bmatrix} U_k Q & V_k Q \\ \bar{U}_k Q & -\bar{V}_k Q \end{bmatrix} \begin{bmatrix} 0 & D_k \\ I_k & 0 \end{bmatrix} + \beta_k \begin{bmatrix} u_{k+1} \\ \bar{u}_{k+1} \end{bmatrix} \begin{bmatrix} 0 & e_k^* Q \end{bmatrix}, \quad (10)$$

or, defining $\hat{U}_k := U_k Q$, $\hat{V}_k := V_k Q$ and $b := \beta_k Q^* e_k$,

$$H \begin{bmatrix} \hat{U}_k & \hat{V}_k \\ \hat{\bar{U}}_k & -\hat{\bar{V}}_k \end{bmatrix} = \begin{bmatrix} \hat{U}_k & \hat{V}_k \\ \hat{\bar{U}}_k & -\hat{\bar{V}}_k \end{bmatrix} \begin{bmatrix} 0 & D_k \\ I_k & 0 \end{bmatrix} + \begin{bmatrix} u_{k+1} \\ \bar{u}_{k+1} \end{bmatrix} \begin{bmatrix} 0 & b^* \end{bmatrix}, \quad (11)$$

Since D_k is diagonal, the previous decomposition can be truncated so that each side of the equality contains only $2r$ columns, with $r < k$. Before truncating, we permute the eigendecomposition of T_k so that the leading block of D_k contains the wanted eigenvalues, i.e., the smallest ones.

After truncation, the decomposition (11) can be extended again to $2k$ columns, by running algorithm 2, which is a modified version of algorithm 1 that receives vectors $[\hat{u}_1, \dots, \hat{u}_r, u_{k+1}]$ and $[\hat{v}_1, \dots, \hat{v}_r, v_{k+1}]$ as the columns of U_{r+1} and V_{r+1} , respectively, and the vector $b = [b_1, \dots, b_r]^T$. Note that vector \tilde{u}_{r+2} , generated in the first iteration of the algorithm, must be orthogonalized against all the columns of U_r , using b_1, \dots, b_r as the orthogonalization coefficients. Algorithm 2 is a generalization of algorithm 1, so it can also be used for the Lanczos process before the first restart, setting $r = 0$ and $b = []$.

ALGORITHM 2: Shao's Lanczos with reorthogonalization and accommodating restart

Input: A definite $2n \times 2n$ BSE matrix H with structure (1); initial vectors in columns of U_{r+1} and V_{r+1} ; vector b ; number of Lanczos steps k .

Output: U_k, V_k, T_k extending decomposition (11) to $2k$ columns.

```

1: for  $j = r + 1, r + 2, \dots, k$  do
2:    $x = Rv_j - C\bar{v}_j$ 
3:    $\tilde{\alpha}_j = \text{Re}(v_j^* x)$ 
4:   if  $j = r + 1$  then
5:      $\tilde{u}_{j+1} = x - U_r b - \tilde{\alpha}_j u_j$ 
6:   else
7:      $\tilde{u}_{j+1} = x - \beta_{j-1} u_{j-1} - \tilde{\alpha}_j u_j$ 
8:   end if
9:    $c = \text{Re}(V_j^* \tilde{u}_{j+1}), \quad d = \text{Im}(U_j^* \tilde{u}_{j+1})i$ 
10:   $\alpha_j = \tilde{\alpha}_j + c_j$ 
11:   $\check{u}_{j+1} = \tilde{u}_{j+1} - U_j c - V_j d$ 
12:   $\check{v}_{j+1} = R\check{u}_{j+1} + C\overline{\check{u}_{j+1}}$ 
13:   $\beta_j = \sqrt{\text{Re}(\check{u}_{j+1}^* \check{v}_{j+1})}$ 
14:   $u_{j+1} = \check{u}_{j+1}/\beta_j, \quad v_{j+1} = \check{v}_{j+1}/\beta_j$ 
15: end for
```

This process is repeated until the desired number of Ritz pairs have converged. We will see below that the entries of b are related to residual norms of each Ritz pair.

3.1.4 Obtaining approximate eigentriplets

It remains to see how to obtain the approximate eigenvalues and eigenvectors from the Krylov decomposition (11). Applying a perfect shuffle symmetric permutation $[e_1, e_{k+1}, e_2, e_{k+2}, \dots]$, the projected matrix

$$\begin{bmatrix} 0 & D_k \\ I_k & 0 \end{bmatrix}$$

gets transformed into a block diagonal matrix with 2×2 diagonal blocks of the form $\begin{bmatrix} 0 & d_i \\ 1 & 0 \end{bmatrix}$ with $d_i > 0$. Each such block admits the eigendecomposition

$$\begin{bmatrix} 0 & d_i \\ 1 & 0 \end{bmatrix} \begin{bmatrix} \sqrt{d_i} & -\sqrt{d_i} \\ 1 & 1 \end{bmatrix} = \begin{bmatrix} \sqrt{d_i} & -\sqrt{d_i} \\ 1 & 1 \end{bmatrix} \begin{bmatrix} \sqrt{d_i} & 0 \\ 0 & -\sqrt{d_i} \end{bmatrix}.$$

Thus, the projected matrix admits the eigendecomposition

$$\begin{bmatrix} 0 & D_k \\ I_k & 0 \end{bmatrix} G = G \begin{bmatrix} D_k^{\frac{1}{2}} & 0 \\ 0 & -D_k^{\frac{1}{2}} \end{bmatrix},$$

where

$$G := \begin{bmatrix} D_k^{\frac{1}{2}} & D_k^{\frac{1}{2}} \\ I_k & -I_k \end{bmatrix}.$$

Substituting in (11) and multiplying on the right by G , we get

$$H \begin{bmatrix} \tilde{X}_1 & \overline{\tilde{X}_2} \\ \tilde{X}_2 & \overline{\tilde{X}_1} \end{bmatrix} = \begin{bmatrix} \tilde{X}_1 & \overline{\tilde{X}_2} \\ \tilde{X}_2 & \overline{\tilde{X}_1} \end{bmatrix} \begin{bmatrix} \tilde{\Lambda}_+ & 0 \\ 0 & -\tilde{\Lambda}_+ \end{bmatrix} + \begin{bmatrix} u_{k+1} \\ \bar{u}_{k+1} \end{bmatrix} \begin{bmatrix} b^* & -b^* \end{bmatrix}, \quad (12)$$

where we use the definitions

$$\tilde{X} = \begin{bmatrix} \tilde{X}_1 & \overline{\tilde{X}_2} \\ \tilde{X}_2 & \overline{\tilde{X}_1} \end{bmatrix} := \begin{bmatrix} \hat{U}_k & \hat{V}_k \\ \hat{U}_k & -\hat{V}_k \end{bmatrix} G, \quad \tilde{\Lambda}_+ := D_k^{\frac{1}{2}}.$$

Clearly, $\tilde{\Lambda}_+$ and \tilde{X} contain approximations to a subset of eigenvalues of H and the corresponding right eigenvectors, respectively. Approximations to left eigenvectors \tilde{Y} can be obtained trivially from \tilde{X} taking into account (7).

Considering column $i \leq k$ of the relation (12), we can see that the residual norm of the approximate eigenpair $(\tilde{\lambda}_i, \tilde{x}_i)$ can be obtained as $\|H\tilde{x}_i - \tilde{\lambda}_i\tilde{x}_i\|_2 = \rho|b_i|$, where $\rho = \|[u_{k+1}^*, \bar{u}_{k+1}^*]^*\|_2$, and we have exactly the same residual norm for the corresponding negative eigenpair in column $i + k$. We consider that an eigenpair is converged when $|b_i| < \text{tol}$ for a given tolerance tol , disregarding ρ . More precisely, we check for convergence in order, i.e., if the number of wanted eigenvalues is n_{ev} , the computation will stop whenever the first $n_{\text{ev}}/2$ residual norms are below the tolerance. Note that the method returns $n_{\text{ev}}/2$ positive eigenvalues together with the same amount of negative ones.

The previous paragraph considers the absolute error of the approximate eigenpair. An alternative is to use the relative residual estimates $|b_i|/|\tilde{\lambda}_i|$, where we are assuming that the approximate eigenvector has been normalized so that $\|\tilde{x}_i\|_2 = 1$ (see section 4 for a discussion about normalization of eigenvectors). In our implementation, the default is to use a relative convergence criterion, but the user can easily switch to an absolute one if preferred.

The overall restarted method is illustrated in algorithm 3.

ALGORITHM 3: Restarted Shao's Lanczos method

Input: A definite $2n \times 2n$ BSE matrix H with structure (1); initial vector \tilde{u}_1 of size n ; maximum number of Lanczos steps k , restart parameter r , number of wanted eigenvalues n_{ev} , tolerance tol .

Output: Approximate eigenpairs $(\tilde{\lambda}_i, \tilde{x}_i)$, $i = 1, \dots, n_{\text{ev}}/2$

1: **repeat**

2: Build Lanczos relation of order k with algorithm 2

3: Compute sorted eigendecomposition $T_k = QD_kQ^*$

4: Update Lanczos relation as in (10)

5: Truncate Lanczos relation to order r as in (11)

6: Set n_{conv} such that $|b_i| < \text{tol} \cdot |\tilde{\lambda}_i|$, $i = 1, \dots, n_{\text{conv}}$

7: **until** $n_{\text{conv}} \geq n_{\text{ev}}/2$

8: Compute eigendecomposition of $\begin{bmatrix} 0 & D_k \\ I_k & 0 \end{bmatrix}$, update Lanczos relation as in (12)

3.2 Method based on Grüning *et al*

3.2.1 Lanczos recurrence

The method proposed in [15] is a Lanczos iteration with an inner product with \hat{H} , although it is reformulated in terms of a much cheaper inner product with the diagonal matrix S , taking into account that $\hat{H} = SH = H^*S$. In particular, for a vector basis $V_j = [v_1, v_2, \dots, v_j]$, the orthogonalization of a new vector $\tilde{v}_{j+1} = Hv_j$ against the previously computed V_j requires computing the inner product $(\tilde{v}_{j+1}, V_j)_{\hat{H}} = (Hv_j, HV_j)_S$. In the Lanczos iteration, HV_j is not computed for every inner product. Instead, it is stored in memory and a new vector is appended at each iteration as it is computed.

Further optimization is possible using an initial vector with the structure $v_1 = \begin{bmatrix} m_1 \\ \bar{m}_1 \end{bmatrix}$, as the (non-restarted) Lanczos algorithm produces a sequence of vectors with the form

$$V_{2k} = \begin{bmatrix} m_1 & n_1 & m_2 & n_2 & \cdots & m_k & n_k \\ \bar{m}_1 & -\bar{n}_1 & \bar{m}_2 & -\bar{n}_2 & \cdots & \bar{m}_k & -\bar{n}_k \end{bmatrix},$$

and a tridiagonal matrix T_{2k} with zeros on the diagonal,

$$T_{2k} = \text{tridiag} \begin{Bmatrix} \hat{\beta}_1 & \hat{\beta}_{k+1} & \hat{\beta}_2 & \cdots & \hat{\beta}_{2k-1} & \hat{\beta}_k \\ 0 & 0 & 0 & \cdots & 0 & 0 \\ \hat{\beta}_1 & \hat{\beta}_{k+1} & \hat{\beta}_2 & \cdots & \hat{\beta}_{2k-1} & \hat{\beta}_k \end{Bmatrix},$$

satisfying the relation

$$HV_{2k} = V_{2k}T_{2k} + \hat{\beta}_{2k}v_{2k+1}e_{2k}^*. \quad (13)$$

Postmultiplying the factorization (13) by an odd-even permutation matrix gives the resulting Lanczos-type relationship

$$H \begin{bmatrix} M_k & N_k \\ \bar{M}_k & -\bar{N}_k \end{bmatrix} = \begin{bmatrix} M_k & N_k \\ \bar{M}_k & -\bar{N}_k \end{bmatrix} \begin{bmatrix} 0 & L_k \\ L_k^* & 0 \end{bmatrix} + \hat{\beta}_{2k} \begin{bmatrix} m_{k+1} \\ \bar{m}_{k+1} \end{bmatrix} e_{2k}^*, \quad (14)$$

where $M_k, N_k \in \mathbb{C}^{n \times k}$, $M_k = [m_1, \dots, m_k]$, $N_k = [n_1, \dots, n_k]$, and L_k is the real lower bidiagonal positive matrix

$$L_k = \begin{bmatrix} \hat{\beta}_1 & & & & \\ \hat{\beta}_{k+1} & \hat{\beta}_2 & & & \\ & \hat{\beta}_{k+2} & \hat{\beta}_3 & & \\ & & \ddots & \ddots & \\ & & & \hat{\beta}_{2k-1} & \hat{\beta}_k \end{bmatrix}.$$

Lanczos vectors satisfy the orthogonality condition

$$\begin{bmatrix} M_k & N_k \\ \bar{M}_k & -\bar{N}_k \end{bmatrix}^* \hat{H} \begin{bmatrix} M_k & N_k \\ \bar{M}_k & -\bar{N}_k \end{bmatrix} = I_{2k},$$

which can also be expressed as

$$\begin{bmatrix} M'_k & N'_k \\ -\bar{M}'_k & \bar{N}'_k \end{bmatrix}^* S \begin{bmatrix} M_k & N_k \\ \bar{M}_k & -\bar{N}_k \end{bmatrix} = I_{2k}, \quad (15)$$

where $M'_k = RM_k + C\bar{M}_k$ and $N'_k = RN_k - C\bar{N}_k$.

Relation (14) is also described in [30, §4.4], where the authors show it is mathematically equivalent to Lanczos relationship (8), with $M_k = \frac{1}{\sqrt{2}}U_k$, $N_k = \frac{1}{\sqrt{2}}V_kL_k^{-*}$, and L_k the Cholesky

factor of T_k . In particular, it is easy to see that relation (14) can be derived from (8), using the similarity transformation

$$\begin{bmatrix} & T_k \\ I_k & \end{bmatrix} = \begin{bmatrix} I_k & \\ & L_k^{-*} \end{bmatrix} \begin{bmatrix} & L_k \\ L_k^* & \end{bmatrix} \begin{bmatrix} I_k & \\ & L_k^* \end{bmatrix},$$

by substituting in (8) and multiplying on the right by $\frac{1}{\sqrt{2}} \begin{bmatrix} I_k & \\ & L_k^{-*} \end{bmatrix}$.

In order to derive the algorithm, assume m_j, m'_j, n_{j-1} and $\hat{\beta}_{k+j-1}$ are available for a given $j \geq 1$, with $n_0 = 0$. From column j of (14),

$$\hat{\beta}_j \begin{bmatrix} n_j \\ -\bar{n}_j \end{bmatrix} = H \begin{bmatrix} m_j \\ \bar{m}_j \end{bmatrix} - \hat{\beta}_{k+j-1} \begin{bmatrix} n_{j-1} \\ -\bar{n}_{j-1} \end{bmatrix},$$

thus,

$$\hat{\beta}_j n_j = m'_j - \hat{\beta}_{k+j-1} n_{j-1},$$

whereby we can compute $\tilde{n}_j = \hat{\beta}_j n_j$, and then normalize to obtain n_j and n'_j ,

$$n_j = \tilde{n}_j / \hat{\beta}_j, \quad n'_j = x_j / \hat{\beta}_j,$$

with $x_j = R\tilde{n}_j - C\bar{\tilde{n}}_j$ and $\hat{\beta}_j = \sqrt{2\text{Re}(\tilde{n}_j^* x_j)}$.

Similarly, from column $k+j$ of (14),

$$\hat{\beta}_{k+j} m_{j+1} = n'_j - \hat{\beta}_j m_j,$$

which we can use to compute $\tilde{m}_{j+1} = \hat{\beta}_{k+j} m_{j+1}$, and normalize to obtain m_{j+1} and m'_{j+1} ,

$$m_{j+1} = \tilde{m}_{j+1} / \hat{\beta}_{k+j}, \quad m'_{j+1} = y_{j+1} / \hat{\beta}_{k+j},$$

with $y_{j+1} = R\tilde{m}_{j+1} + C\bar{\tilde{m}}_{j+1}$ and $\hat{\beta}_{k+j} = \sqrt{2\text{Re}(\tilde{m}_{j+1}^* y_{j+1})}$.

An initial vector m_1 can be generated from an arbitrary \tilde{m}_1 , by computing y_1 and normalizing,

$$m_1 = \tilde{m}_1 / \hat{\beta}_0, \quad \text{with } \hat{\beta}_0 = \sqrt{2\text{Re}(\tilde{m}_1^* y_1)}.$$

Further details of the method can be found in [15, 30].

Bases M'_k and N'_k are constructed explicitly in our method as they are used in the reorthogonalization. Because of that, memory requirements for this method are larger than for the other two methods, as the number of vectors to keep doubles.

3.2.2 Reorthogonalization

Similarly to Shao's method, to accurately compute the eigenvectors it is important to guarantee the orthogonality of the generated vectors. This requires performing a reorthogonalization against the full basis after the local orthogonalization described above.

Assuming orthogonality of vector \tilde{m}_{j+1} is not perfect, we can write

$$\hat{\beta}_{k+j} \begin{bmatrix} m_{j+1} \\ \bar{m}_{j+1} \end{bmatrix} = \begin{bmatrix} \tilde{m}_{j+1} \\ \bar{\tilde{m}}_{j+1} \end{bmatrix} - \begin{bmatrix} M_j & N_j \\ \bar{M}_j & -\bar{N}_j \end{bmatrix} \begin{bmatrix} c \\ d \end{bmatrix}.$$

Premultiplying by $\begin{bmatrix} M'_j & N'_j \\ -\bar{M}'_j & \bar{N}'_j \end{bmatrix}^* S$ and taking into account the orthogonality condition (15),

$$\begin{bmatrix} c \\ d \end{bmatrix} = \begin{bmatrix} M'_j & N'_j \\ -\bar{M}'_j & \bar{N}'_j \end{bmatrix}^* S \begin{bmatrix} \tilde{m}_{j+1} \\ \bar{\tilde{m}}_{j+1} \end{bmatrix},$$

which leads to

$$\begin{aligned} c &= 2\text{Re}(M_j'^* \tilde{m}_{j+1}), \\ d &= 2\text{Im}(N_j'^* \tilde{m}_{j+1})i. \end{aligned}$$

After computing c, d , a reorthogonalized vector \tilde{m}_{j+1} is obtained as

$$\tilde{m}_{j+1} = \hat{\beta}_{k+j} m_{j+1} = \tilde{m}_{j+1} - M_j c - N_j d.$$

Our results indicate that ensuring orthogonality of each new vector m_{j+1} with respect to M_j and N_j is enough to also keep orthogonality of vectors n_j . This is in line with what happens with the Lanczos bidiagonalization process [32], and comes from the fact that vector bases M_k and N_k are closely related.

3.2.3 Restart

The restart must preserve the structure of the vector bases. Let $L_k = Q \Sigma_k P^*$ be the SVD of L_k , with Q and P orthogonal. Then

$$\begin{bmatrix} 0 & L_k \\ L_k^* & 0 \end{bmatrix} = \begin{bmatrix} Q & 0 \\ 0 & P \end{bmatrix} \begin{bmatrix} 0 & \Sigma_k \\ \Sigma_k & 0 \end{bmatrix} \begin{bmatrix} Q^* & 0 \\ 0 & P^* \end{bmatrix}.$$

Substituting in (14) and multiplying on the right by $\begin{bmatrix} Q & 0 \\ 0 & P \end{bmatrix}$ we get

$$H \begin{bmatrix} M_k Q & N_k P \\ \overline{M_k Q} & -\overline{N_k P} \end{bmatrix} = \begin{bmatrix} M_k Q & N_k P \\ \overline{M_k Q} & -\overline{N_k P} \end{bmatrix} \begin{bmatrix} 0 & \Sigma_k \\ \Sigma_k & 0 \end{bmatrix} + \hat{\beta}_{2k} \begin{bmatrix} m_{k+1} \\ \overline{m_{k+1}} \end{bmatrix} \begin{bmatrix} 0 & e_k^* P \end{bmatrix},$$

or, defining $\hat{M}_k := M_k Q, \hat{N}_k := N_k P$ and $b := \hat{\beta}_{2k} P^* e_k$,

$$H \begin{bmatrix} \hat{M}_k & \hat{N}_k \\ \overline{\hat{M}_k} & -\overline{\hat{N}_k} \end{bmatrix} = \begin{bmatrix} \hat{M}_k & \hat{N}_k \\ \overline{\hat{M}_k} & -\overline{\hat{N}_k} \end{bmatrix} \begin{bmatrix} 0 & \Sigma_k \\ \Sigma_k & 0 \end{bmatrix} + \begin{bmatrix} m_{k+1} \\ \overline{m_{k+1}} \end{bmatrix} \begin{bmatrix} 0 & b^* \end{bmatrix}. \quad (16)$$

ALGORITHM 4: Grüning's Lanczos with reorthogonalization

Input: A definite $2n \times 2n$ BSE matrix H with structure (1); vector bases M_{r+1}, M'_{r+1}, N_r and N'_r ; bidiagonal L_r with nonzero entries $\hat{\beta}_1, \dots, \hat{\beta}_r, \hat{\beta}_{k+1}, \dots, \hat{\beta}_{k+r}$; vector b ; number of Lanczos steps k .

Output: $M_{k+1}, M'_{k+1}, N_k, N'_k, L_k$, extending decomposition (16) to $2k$ columns.

```

1: for  $j = r + 1, r + 2, \dots, k$  do
2:   if  $j = r + 1$  then
3:      $\tilde{n}_j = m'_j - N_r b$ 
4:   else
5:      $\tilde{n}_j = m'_j - n_{j-1} \hat{\beta}_{k+j-1}$ 
6:   end if
7:    $x = R \tilde{n}_j - C \tilde{\tilde{n}}_j$ 
8:    $\hat{\beta}_j = \sqrt{2\text{Re}(\tilde{n}_j^* x)}$ 
9:    $n_j = \tilde{n}_j / \hat{\beta}_j, \quad n'_j = x / \hat{\beta}_j$ 
10:   $\tilde{m}_{j+1} = n'_j - m_j \hat{\beta}_j$ 
11:   $c = 2\text{Re}(M_j'^* \tilde{m}_{j+1}), \quad d = 2\text{Im}(N_j'^* \tilde{m}_{j+1})i, \quad \tilde{m}_{j+1} = \tilde{m}_{j+1} - M_j c - N_j d$ 
12:   $x = R \tilde{m}_{j+1} + C \tilde{\tilde{m}}_{j+1}$ 
13:   $\hat{\beta}_{k+j} = \sqrt{2\text{Re}(\tilde{m}_{j+1}^* x)}$ 
14:   $m_{j+1} = \tilde{m}_{j+1} / \hat{\beta}_{k+j}, \quad m'_{j+1} = x / \hat{\beta}_{k+j}$ 
15: end for
```

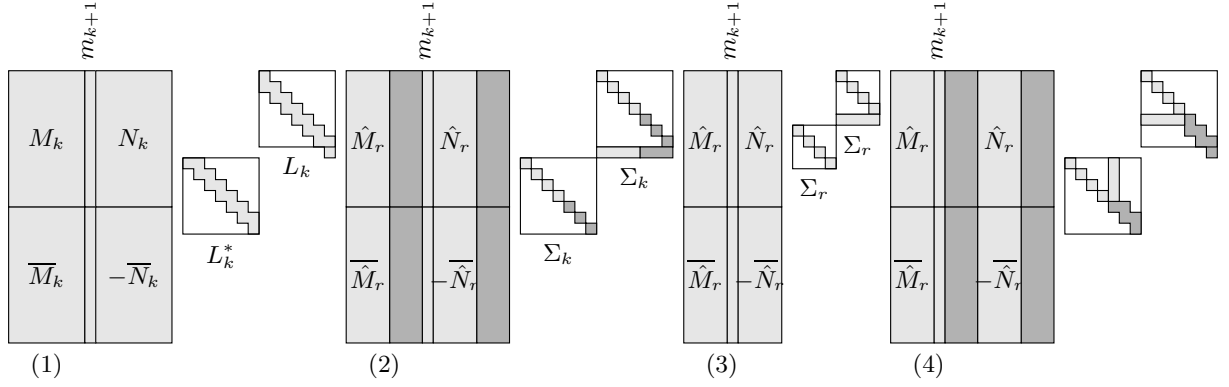


Figure 1: Illustration of the steps of thick restart in the Grüning method: (1) initial Lanczos factorization of order k , (2) solve projected problem, sort and check convergence, (3) truncate to factorization of order r , and (4) extend to a factorization of order k .

We assume the SVD decomposition of L_k has been sorted so that the first elements in the diagonal of Σ_k correspond to the smallest singular values. This decomposition is then truncated to $2r$ columns, with $r < k$, and then the process is restarted, extending the decomposition to $2k$ columns by means of Algorithm 4, which also details the reorthogonalization process described in section 3.2.2. We repeat this process, extending and truncating until the desired number of Ritz eigenvalues have converged.

The steps of the restart process are better visualized in fig. 1. The special orthogonalization with vector b is considered in step 4. This can also be seen in algorithm 4.

3.2.4 Obtaining the eigenvectors

To obtain the eigenvalues and eigenvectors, we take the Krylov factorization (16) and define

$$\hat{G} := \frac{1}{\sqrt{2}} \begin{bmatrix} I_k & I_k \\ I_k & -I_k \end{bmatrix}, \quad (17)$$

so that

$$\begin{bmatrix} 0 & \Sigma_k \\ \Sigma_k & 0 \end{bmatrix} = \hat{G} \begin{bmatrix} \Sigma_k & 0 \\ 0 & -\Sigma_k \end{bmatrix} \hat{G}^*.$$

Substituting this equality in (16) and multiplying on the right by \hat{G} yields

$$H \begin{bmatrix} \tilde{X}_1 & \overline{\tilde{X}}_2 \\ \tilde{X}_2 & \overline{\tilde{X}}_1 \end{bmatrix} = \begin{bmatrix} \tilde{X}_1 & \overline{\tilde{X}}_2 \\ \tilde{X}_2 & \overline{\tilde{X}}_1 \end{bmatrix} \begin{bmatrix} \tilde{\Lambda}_+ & 0 \\ 0 & -\tilde{\Lambda}_+ \end{bmatrix} + \frac{1}{\sqrt{2}} \begin{bmatrix} m_{k+1} \\ \overline{m}_{k+1} \end{bmatrix} \begin{bmatrix} b^* & -b^* \end{bmatrix},$$

where we use the following definitions, corresponding to the approximate eigenpairs:

$$\begin{bmatrix} \tilde{X}_1 & \overline{\tilde{X}}_2 \\ \tilde{X}_2 & \overline{\tilde{X}}_1 \end{bmatrix} := \begin{bmatrix} \hat{M}_k & \hat{N}_k \\ \hat{M}_k & -\hat{N}_k \end{bmatrix} \hat{G} = \frac{1}{\sqrt{2}} \begin{bmatrix} \hat{M}_k + \hat{N}_k & \hat{M}_k - \hat{N}_k \\ \hat{M}_k - \hat{N}_k & \hat{M}_k + \hat{N}_k \end{bmatrix}, \quad \tilde{\Lambda}_+ := \Sigma_k.$$

The product with $\frac{1}{\sqrt{2}}$ is not required, because the eigenvectors can be normalized in different ways. The normalization of the vectors will be discussed in section 4. The left eigenvectors are computed as in (7).

3.3 Method resulting in a Bethe–Salpeter projected eigenproblem

3.3.1 Lanczos recurrence

In [30, §4.4], the authors mention a reformulation of the Lanczos relation where the projected matrix also has Bethe–Salpeter structure. Here we work out the details of a restarted solver based on this formulation. We start by stating a proposition showing the equivalence between the two Lanczos decompositions [30, §4.4].

Proposition 1. *The Lanczos-type relation*

$$H \begin{bmatrix} W_k & \overline{Z}_k \\ Z_k & \overline{W}_k \end{bmatrix} = \begin{bmatrix} W_k & \overline{Z}_k \\ Z_k & \overline{W}_k \end{bmatrix} \begin{bmatrix} A_k & B_k \\ -B_k & -A_k \end{bmatrix} + \frac{1}{2}\beta_k \begin{bmatrix} w_{k+1} & \bar{z}_{k+1} \\ z_{k+1} & \bar{w}_{k+1} \end{bmatrix} \begin{bmatrix} e_k^* & -e_k^* \\ e_k^* & -e_k^* \end{bmatrix}, \quad (18)$$

where

$$W_{k+1} := \frac{U_{k+1} + V_{k+1}}{2}, \quad Z_{k+1} := \frac{\overline{U}_{k+1} - \overline{V}_{k+1}}{2}, \quad A_k := \frac{I + T_k}{2}, \quad B_k := \frac{I - T_k}{2},$$

is equivalent to (8) in the sense that both provide the same Ritz approximations.

Proof. The proof is based on the similarity transformation

$$\begin{bmatrix} & T_k \\ I_k & \end{bmatrix} = \hat{G} \begin{bmatrix} A_k & B_k \\ -B_k & -A_k \end{bmatrix} \hat{G},$$

where $\hat{G} = \hat{G}^{-1} = \frac{1}{\sqrt{2}} \begin{bmatrix} I_k & I_k \\ I_k & -I_k \end{bmatrix}$ as defined in (17).

Substituting in (8) and multiplying on the right by $\frac{1}{\sqrt{2}}\hat{G}$, we get the relation (18)¹. It follows that the Ritz approximations provided by (18) and (8) are the same. \square

From the relation with the vector bases of Shao’s method, we can easily check that the orthogonality condition is

$$\begin{bmatrix} W_k & -\overline{Z}_k \\ -Z_k & \overline{W}_k \end{bmatrix}^* \begin{bmatrix} W_k & \overline{Z}_k \\ Z_k & \overline{W}_k \end{bmatrix} = I_{2k}, \quad (19)$$

or

$$\begin{bmatrix} W_k & \overline{Z}_k \\ Z_k & \overline{W}_k \end{bmatrix}^* \begin{bmatrix} I_n & \\ & -I_n \end{bmatrix} \begin{bmatrix} W_k & \overline{Z}_k \\ Z_k & \overline{W}_k \end{bmatrix} = \begin{bmatrix} I_k & \\ & -I_k \end{bmatrix}. \quad (20)$$

To derive the algorithm, we have to consider (18) as a kind of block Lanczos-type relation with two initial vectors. We use the notation

$$A_k = \text{tridiag} \begin{bmatrix} \beta_1/2 & \cdots & \beta_{k-1}/2 \\ a_1 & \cdots & a_k \\ \beta_1/2 & \cdots & \beta_{k-1}/2 \end{bmatrix},$$

$$B_k = \text{tridiag} \begin{bmatrix} -\beta_1/2 & \cdots & -\beta_{k-1}/2 \\ b_1 & \cdots & b_k \\ -\beta_1/2 & \cdots & -\beta_{k-1}/2 \end{bmatrix},$$

with $a_i = (1 + \alpha_i)/2$, $b_i = (1 - \alpha_i)/2$, $i = 1, \dots, k$.

In each iteration j of the method we start with vectors u_j, v_j corresponding to Shao’s method, as well as vectors w_{j-1}, z_{j-1}, w_j and z_j , and we compute vectors u_{j+1}, v_{j+1} and w_{j+1}, z_{j+1} . Vectors u_j, v_j are discarded once the iteration is complete.

¹The last term in (18) differs from the one given in [30, §4.4], which we believe is wrong.

Equating column j ($j = 2, \dots, k$) in both sides of (18) results in

$$\begin{bmatrix} w'_j \\ z'_j \end{bmatrix} = \frac{\beta_{j-1}}{2} \begin{bmatrix} w_{j-1} + \bar{z}_{j-1} \\ z_{j-1} + \bar{w}_{j-1} \end{bmatrix} + a_j \begin{bmatrix} w_j \\ z_j \end{bmatrix} + (a_j - 1) \begin{bmatrix} \bar{z}_j \\ \bar{w}_j \end{bmatrix} + \frac{\beta_j}{2} \begin{bmatrix} w_{j+1} + \bar{z}_{j+1} \\ \bar{w}_{j+1} + z_{j+1} \end{bmatrix}, \quad (21)$$

where

$$\begin{bmatrix} w'_j \\ z'_j \end{bmatrix} = H \begin{bmatrix} w_j \\ z_j \end{bmatrix}.$$

Note that equating column $j + k$ gives the same vectors, but swapped, conjugated and with the sign changed. Multiplying on the left by $[w_j^*, -z_j^*]$ and taking into account orthogonality condition (19), yields

$$a_j = \begin{bmatrix} w_j \\ -z_j \end{bmatrix}^* \begin{bmatrix} w'_j \\ z'_j \end{bmatrix}.$$

Vectors w'_j and z'_j can be computed efficiently using v_j . Equation (8) from Shao's method implies

$$\begin{bmatrix} v_j \\ -\bar{v}_j \end{bmatrix} = H \begin{bmatrix} u_j \\ \bar{u}_j \end{bmatrix}. \quad (22)$$

Using that, we get

$$\begin{bmatrix} w'_j \\ z'_j \end{bmatrix} = \frac{1}{2} H \begin{bmatrix} u_j + v_j \\ \bar{u}_j - \bar{v}_j \end{bmatrix} = \frac{1}{2} \left(\begin{bmatrix} v_j \\ -\bar{v}_j \end{bmatrix} + H \begin{bmatrix} v_j \\ -\bar{v}_j \end{bmatrix} \right).$$

Thus,

$$w'_j = \frac{1}{2}(v_j + v'_j), \quad z'_j = \frac{1}{2}(\overline{v'_j - v_j}),$$

where

$$v'_j = Rv_j - C\bar{v}_j.$$

In the relation (21) there are two unknowns, w_{j+1} and z_{j+1} . If we express them in terms of u_{k+1} , it is possible to isolate them,

$$\frac{1}{2}\beta_j \begin{bmatrix} u_{j+1} \\ \bar{u}_{j+1} \end{bmatrix} = \begin{bmatrix} w'_j - \frac{1}{2}\beta_{j-1}(w_{j-1} + \bar{z}_{j-1}) - a_j w_j - (a_j - 1)\bar{z}_j \\ z'_j - \frac{1}{2}\beta_{j-1}(z_{j-1} + \bar{w}_{j-1}) - a_j z_j - (a_j - 1)\bar{w}_j \end{bmatrix}.$$

We only need the upper block of the equality to compute $\tilde{u}_{j+1} = \frac{1}{2}\beta_j u_{j+1}$. From that, we compute $\beta_j, u_{j+1}, v_{j+1}$, using (22) and taking into account that, from the formulation of Shao's method, we have

$$\begin{bmatrix} u_{j+1} \\ -\bar{u}_{j+1} \end{bmatrix}^* \begin{bmatrix} v_{j+1} \\ -\bar{v}_{j+1} \end{bmatrix} = 2.$$

If we compute

$$\tilde{v}_{j+1} = R\tilde{u}_{j+1} + C\bar{\tilde{u}}_{j+1},$$

we have that

$$\begin{bmatrix} \tilde{u}_{j+1} \\ -\bar{\tilde{u}}_{j+1} \end{bmatrix}^* \begin{bmatrix} \tilde{v}_{j+1} \\ -\bar{\tilde{v}}_{j+1} \end{bmatrix} = \frac{1}{2}\beta_j^2 \implies \beta_j = 2\sqrt{\text{Re}(\tilde{u}_{j+1}^* \tilde{v}_{j+1})},$$

$$u_{j+1} = \frac{2}{\beta_j} \tilde{u}_{j+1}, \quad v_{j+1} = \frac{2}{\beta_j} \tilde{v}_{j+1},$$

and finally we compute the next vectors w_{j+1}, z_{j+1} , which ends the iteration,

$$w_{j+1} = \frac{u_{j+1} + v_{j+1}}{2}, \quad z_{j+1} = \frac{\bar{u}_{j+1} - \bar{v}_{j+1}}{2}.$$

3.3.2 Reorthogonalization

To derive the reorthogonalization coefficients, we consider the equality,

$$\frac{1}{2}\beta_j \begin{bmatrix} u_{j+1} \\ \bar{u}_{j+1} \end{bmatrix} = \begin{bmatrix} \tilde{u}_{j+1} \\ \bar{\tilde{u}}_{j+1} \end{bmatrix} - \begin{bmatrix} W_j & \bar{Z}_j \\ Z_j & \bar{W}_j \end{bmatrix} \begin{bmatrix} c \\ d \end{bmatrix}.$$

Premultiplying by

$$\begin{bmatrix} W_j & -\bar{Z}_j \\ -Z_j & \bar{W}_j \end{bmatrix}^*$$

and taking into account the orthogonality condition (19), we have

$$\begin{bmatrix} c \\ d \end{bmatrix} = \begin{bmatrix} W_j & -\bar{Z}_j \\ -Z_j & \bar{W}_j \end{bmatrix}^* \begin{bmatrix} \tilde{u}_{j+1} \\ \bar{\tilde{u}}_{j+1} \end{bmatrix}, \quad (23)$$

resulting in,

$$c = \bar{d} = W_j \tilde{u}_{j+1} - \bar{Z}_j \bar{\tilde{u}}_{j+1}.$$

We can then obtain a reorthogonalized vector \tilde{u}_{j+1} as

$$\tilde{u}_{j+1} = \frac{1}{2}\beta_j u_{j+1} = \tilde{u}_{j+1} - W_j c - \bar{Z}_j \bar{c}.$$

ALGORITHM 5: Projected BSE method with reorthogonalization

Input: A definite $2n \times 2n$ BSE matrix H with structure (1); initial vectors in columns of W_{r+1} and Z_{r+1} ; vector b ; number of Lanczos steps k .

Output: W_k, Z_k, T_k making up Lanczos-type decomposition (18).

```

1:  $v = w_{r+1} - \bar{z}_{r+1}$ 
2: for  $j = r+1, r+2, \dots, k$  do
3:    $v' = Rv - C\bar{v}$ 
4:    $w' = (v' + v)/2, \quad z' = (\overline{v' - v})/2$ 
5:    $\tilde{a}_j = w_j^* w' - z_j^* z'$ 
6:   if  $j = r+1$  then
7:      $\tilde{u} = w' - W_r b - \bar{Z}_r \bar{b} - \tilde{a}_j w_j - (\tilde{a}_j - 1)\bar{z}_j$ 
8:   else
9:      $\tilde{u} = w' - \frac{1}{2}\beta_{j-1}(w_{j-1} + \bar{z}_{j-1}) - \tilde{a}_j w_j - (\tilde{a}_j - 1)\bar{z}_j$ 
10:  end if
11:   $c = W_j^* \tilde{u} - Z_j^* \bar{\tilde{u}}$ 
12:   $\tilde{u} = \tilde{u} - W_j c - \bar{Z}_j \bar{c}$ 
13:   $a_j = \tilde{a}_j + c_j, \quad \alpha_j = 2a_j - 1$ 
14:   $\tilde{v} = R\tilde{u} + C\bar{\tilde{u}}$ 
15:   $\beta_j = 2\sqrt{\text{Re}(\tilde{u}^* \tilde{v})}$ 
16:   $u = 2/\beta_j \tilde{u}, \quad v = 2/\beta_j \tilde{v}$ 
17:   $w_{j+1} = (u + v)/2, \quad z_{j+1} = (\overline{u - v})/2$ 
18: end for
```

3.3.3 Restart

The projected matrix $\begin{bmatrix} A_k & B_k \\ -B_k & -A_k \end{bmatrix}$ is real and has a Bethe–Salpeter structure. To restart the Lanczos relation (18), we can exploit the fact that both A_k and B_k depend on T_k , and use its eigendecomposition $T_k = QD_kQ^*$, with Q orthogonal. Then,

$$\begin{bmatrix} A_k & B_k \\ -B_k & -A_k \end{bmatrix} = \frac{1}{2} \begin{bmatrix} I + T_k & I - T_k \\ -I + T_k & -I - T_k \end{bmatrix} = \begin{bmatrix} Q & \\ & Q \end{bmatrix} \frac{1}{2} \begin{bmatrix} I + D_k & I - D_k \\ -(I - D_k) & -(I + D_k) \end{bmatrix} \begin{bmatrix} Q^* & \\ & Q^* \end{bmatrix}.$$

Inserting this into (18) and multiplying on the right by $\begin{bmatrix} Q & 0 \\ 0 & Q \end{bmatrix}$ we arrive at

$$H \begin{bmatrix} W_k Q & \overline{Z}_k Q \\ Z_k Q & \overline{W}_k Q \end{bmatrix} = \begin{bmatrix} W_k Q & \overline{Z}_k Q \\ Z_k Q & \overline{W}_k Q \end{bmatrix} \frac{1}{2} \begin{bmatrix} I + D_k & I - D_k \\ -(I - D_k) & -(I + D_k) \end{bmatrix} + \frac{1}{2} \beta_k \begin{bmatrix} u_{k+1} \\ \bar{u}_{k+1} \end{bmatrix} \begin{bmatrix} e_k^* Q & -e_k^* Q \end{bmatrix},$$

or, defining $\tilde{W}_k := W_k Q$, $\tilde{Z}_k := Z_k Q$,

$$H \begin{bmatrix} \tilde{W}_k & \overline{\tilde{Z}}_k \\ \tilde{Z}_k & \overline{\tilde{W}}_k \end{bmatrix} = \begin{bmatrix} \tilde{W}_k & \overline{\tilde{Z}}_k \\ \tilde{Z}_k & \overline{\tilde{W}}_k \end{bmatrix} \frac{1}{2} \begin{bmatrix} I + D_k & I - D_k \\ -(I - D_k) & -(I + D_k) \end{bmatrix} + \frac{1}{2} \beta_k \begin{bmatrix} u_{k+1} \\ \bar{u}_{k+1} \end{bmatrix} \begin{bmatrix} e_k^* Q & -e_k^* Q \end{bmatrix}. \quad (24)$$

Similarly to the other two methods, this expression can be truncated to $2r$ columns, after reordering to keep the wanted approximate eigenvalues. Then, it can be expanded again to $2k$ columns by means of Algorithm 5.

3.3.4 Obtaining the eigenvectors

It can be easily verified that the eigenvalue decomposition of the projected matrix can be written as

$$\frac{1}{2} \begin{bmatrix} I + D_k & I - D_k \\ -(I - D_k) & -(I + D_k) \end{bmatrix} \tilde{G} = \tilde{G} \begin{bmatrix} D_k^{\frac{1}{2}} & 0 \\ 0 & -D_k^{\frac{1}{2}} \end{bmatrix},$$

where

$$\tilde{G} := \begin{bmatrix} D_k^{\frac{1}{2}} + I & D_k^{\frac{1}{2}} - I \\ D_k^{\frac{1}{2}} - I & D_k^{\frac{1}{2}} + I \end{bmatrix}.$$

With this, if we multiply the relation (24) on the right by \tilde{G} , we obtain

$$H \begin{bmatrix} \tilde{X}_1 & \overline{\tilde{X}}_2 \\ \tilde{X}_2 & \overline{\tilde{X}}_1 \end{bmatrix} = \begin{bmatrix} \tilde{X}_1 & \overline{\tilde{X}}_2 \\ \tilde{X}_2 & \overline{\tilde{X}}_1 \end{bmatrix} \begin{bmatrix} \tilde{\Lambda}_+ & \\ & -\tilde{\Lambda}_+ \end{bmatrix} + \frac{1}{2} \beta_k \begin{bmatrix} u_{k+1} \\ \bar{u}_{k+1} \end{bmatrix} \begin{bmatrix} e_k^* Q \tilde{G} & -e_k^* Q \tilde{G} \end{bmatrix}, \quad (25)$$

where we have defined the approximate eigenpairs as

$$\begin{bmatrix} \tilde{X}_1 & \overline{\tilde{X}}_2 \\ \tilde{X}_2 & \overline{\tilde{X}}_1 \end{bmatrix} := \begin{bmatrix} \tilde{W}_k & \overline{\tilde{Z}}_k \\ \tilde{Z}_k & \overline{\tilde{W}}_k \end{bmatrix} \tilde{G}, \quad \tilde{\Lambda}_+ := D_k^{\frac{1}{2}}.$$

4 Details of the implementation in SLEPc

In this section we discuss a few details related to the implementation of the methods within the SLEPc framework.

User interface To solve a Bethe–Salpeter eigenproblem with SLEPc, the application code has to first create the matrices R and C , as any valid PETSc `Mat` type, and then call `MatCreateBSE(R,C,&H)`. This helper function will create matrix H of (1) as a nested matrix (`MATNEST`) that stores the upper blocks R and C explicitly but handles the bottom blocks in an implicit way.

Once the $2n \times 2n$ matrix H has been created, it is passed to the SLEPc eigensolver as any other matrix. If the problem is solved as a standard non-Hermitian eigenproblem, then the structure will not be taken into account, but if the problem type is set to `EPS_BSE` and the default eigensolver is selected then the structure-preserving solvers presented above will be used. All other features such as stopping criterion, convergence monitor, residual check, etc. work as usual.

Management of basis vectors Every SLEPc eigensolver internally holds a basis of vectors (BV) of the same length as the matrix, i.e., $2n$ in this case. However, the algorithms presented in this paper operate with two bases of length n (e.g., U_k and V_k in the case of algorithm 1). For the internal implementation of these solvers, we have added a new operation `BVGetSplitRows()` that provides a clean way to view the basis of $2n$ -vectors as two stacked bases of n -vectors, including the case when these vectors are distributed across several MPI processes in a parallel computation.

Once the eigensolver has reached convergence, the basis vectors contain all the necessary information to build the right and left eigenvectors as in theorem 1. One remaining thing is how to normalize eigenvectors. We have opted for normalizing them such that $\|x_i\|_2 = 1$ (which implies that also $\|y_i\|_2 = 1$), $i = 1, \dots, n_{\text{ev}}$. This is consistent with the normalization in standard non-Hermitian eigenproblems in SLEPc. An alternative would be to normalize them with respect to the norm induced by \hat{H} or the pseudo-norm induced by the signature S (since eigenvectors are orthogonal with respect to both inner products), but it was not clear if this would be of any use for applications.

Orthogonalization As in any Lanczos-type eigensolver, one can propose sophisticated schemes such as partial reorthogonalization in order to avoid loss of orthogonality among the generated Lanczos vectors when Ritz values begin to stabilize. In SLEPc we tend to avoid this type of strategies, due to the increased complexity of implementation and because for moderate restart size full reorthogonalization is usually not much more expensive. In most SLEPc solvers we use Classical Gram-Schmidt with conditional reorthogonalization [17]. However, the methods of section 3 cannot reuse this procedure directly because the formulas are slightly different. In this case, we have opted for a hybrid scheme where a simple local orthogonalization is followed unconditionally by a full reorthogonalization involving all previously computed Lanczos vectors. This corresponds to lines 6 – 10 of algorithm 1, and similarly in the other methods. In our experiments, we have checked that this scheme is enough to obtain an orthogonal basis to working precision, and does not require an additional orthogonalization in any case.

Shift-and-invert As mentioned in section 2, the discussed methods already approximate the smallest magnitude eigenvalues, which are the relevant ones for applications, without having to apply any kind of spectral transformation. Still, we discuss this possibility here, as it may be useful in case of tightly clustered eigenvalues around zero.

Most SLEPc solvers can be combined with a shift-and-invert technique, which, in the case of standard eigenproblems, will operate with matrix $(A - \sigma I)^{-1}$ to compute eigenvalues closest to σ . The first thing to note is that in the case of Bethe–Salpeter eigensolvers, we must have $\sigma = 0$, otherwise the Bethe–Salpeter structure is lost. It can be easily shown that H^{-1} also has a (definite) Bethe–Salpeter structure. Another comment is that solving linear systems with H using an iterative method such as GMRES is also not viable since again the Bethe–Salpeter structure would not be preserved. We should either build H^{-1} explicitly (possible in the case of dense matrices, but not implemented in SLEPc), or handle H^{-1} implicitly via a Schur complement scheme. The latter can be used in SLEPc via the PETSc preconditioner `PCFIELDSPLIT` selecting the appropriate options, which would involve two factorizations of size n , one for the R block and another one for the Schur complement.

5 Computational results

We now provide some results about accuracy, convergence and computational performance of the proposed methods. The solvers are available in SLEPc since version 3.22. We use version

Table 1: Description of the test problems used in the computational experiments: type of problem (sparse or dense), numerical precision used, dimension n of the R and C blocks, number of requested eigenvalues **nev**, first computed (positive) eigenvalue, and average separation of the first **nev**/2 positive eigenvalues.

name	type	precision	n	nev	first value	sep
pentadiag small	sparse	double	5000	100	2.1503397672	$3.3 \cdot 10^{-5}$
pentadiag large	sparse	double	50000	100	2.1503391439	$3.2 \cdot 10^{-7}$
Crl ₃ small	dense	single	1152	100	0.0518548376	$1.6 \cdot 10^{-4}$
Crl ₃ large	dense	single	11520	100	0.0518094226	$1.6 \cdot 10^{-4}$

3.23, together with PETSc 3.23, built with GNU compilers (version 11.4.0) and MPICH version 4.0. All computational experiments are carried out in complex arithmetic. The computer used has two AMD EPYC GENOA 9354 processors, each of them with 32 physical cores (64 threads) at 3.25 GHz, with 384 GB of main memory (DDR5 at 4800 MHz). The server also includes an AMD Instinct MI210 GPU with 64 GB of HBM2e memory and 6656 stream processors.

Table 1 lists the problems used in the experiments, summarizing some properties and parameters. The first two problems use a synthetic matrix created to exercise the solvers with sparse matrices, but it does not correspond to any real application. The third and fourth problems come from a simulation with the Yambo code, where the matrices are dense. In the case of Yambo, we use single precision arithmetic, which is sufficient for the application requirements and provides substantial memory savings in the case of large problems. Here is a short description of the problems:

- In the **pentadiag** test, both R and C blocks are Toeplitz matrices with only a few nonzero diagonals. More precisely, $R = \text{pentadiag}(a, b, c, \bar{b}, \bar{a})$ and $C = \text{tridiag}(b, d, b)$. In our tests we set the values $a = -0.1 + 0.2i$, $b = 1 + 0.5i$, $c = 4.5$, and $d = 2 + 0.2i$. The tolerance in this case is set to 10^{-8} , the default for double precision.
- Crl₃ (chromium triiodide) is a dense matrix from a Yambo simulation. The size of the blocks R and C is $n_k n_c n_v$ where n_k is related to the size of the grid, n_c is the number of unoccupied states and n_v is the number of occupied states. We work with two cases of different size, with the same value of n_k , but different band intervals, a parameter which modifies n_c and n_v . The band interval is 31-40 for the **small** case and 23-48 for the **large** case. The tolerance for this problem is set to 10^{-5} , the default for single precision.

In all cases, 100 eigenvalues are computed (**nev**). The number of column vectors (**ncv**, which corresponds to k in the algorithms of section 3) is set to twice the number of requested eigenpairs that will be computed by the iterative solver. The methods of section 3 effectively compute half of the requested eigenpairs, which in this case are 50 eigenvalues from the positive side of the spectrum and their eigenvectors, while their negative counterparts are obtained a posteriori. Therefore an **ncv** of 100 is used. For the non-Hermitian method, used for comparison, **ncv** is set to 200, because all 100 requested eigenvalues are computed by the iterative method.

Table 2 presents results of our three new solvers (**shao**, **gruning**, **projectedbs**) as well as non-Hermitian Krylov-Schur for comparison, with executions in both CPU and GPU. The number of restarts required to compute 100 eigenvalues clearly indicates that the **pentadiag** problem is much more difficult compared to Crl₃. The justification is that eigenvalues of **pentadiag** are closer to each other, especially for large dimension. The average separation of the wanted eigenvalues is shown in the last column of table 1. All three structure-preserving methods take approximately the same number of restarts, while the non-Hermitian solver sometimes needs less iterations,

Table 2: Results of the computational experiments in CPU with one MPI process, and in GPU. The solvers are compared in terms of the number of restarts (its), execution time, largest relative residual and bi-orthogonality of the right and left eigenvectors. The non-Hermitian method computes only the right eigenvectors, the left eigenvectors are built as in theorem 1 to check bi-orthogonality.

name	exec	solver	its	time	residual	bi-orthog
pentadiag small	CPU	shao	152	6.48	$2.60 \cdot 10^{-9}$	$1.34 \cdot 10^{-14}$
pentadiag small	CPU	gruning	151	9.9	$5.00 \cdot 10^{-9}$	$2.73 \cdot 10^{-10}$
pentadiag small	CPU	projectedbse	152	6.88	$2.60 \cdot 10^{-9}$	$1.69 \cdot 10^{-14}$
pentadiag small	CPU	non-Hermitian	151	38.52	$9.86 \cdot 10^{-9}$	$5.33 \cdot 10^{-6}$
pentadiag large	CPU	shao	6520	4,778	$2.60 \cdot 10^{-9}$	$8.78 \cdot 10^{-14}$
pentadiag large	CPU	gruning	6613	5,600	$5.72 \cdot 10^{-9}$	$6.23 \cdot 10^{-10}$
pentadiag large	CPU	projectedbse	6537	5,014	$2.59 \cdot 10^{-9}$	$1.05 \cdot 10^{-13}$
pentadiag large	CPU	non-Hermitian	4064	15,418	$9.16 \cdot 10^{-9}$	$2.99 \cdot 10^{-2}$
Crl ₃ small	CPU	shao	16	0.60	$7.74 \cdot 10^{-5}$	$1.97 \cdot 10^{-6}$
Crl ₃ small	CPU	gruning	17	0.75	$5.09 \cdot 10^{-6}$	$3.42 \cdot 10^{-6}$
Crl ₃ small	CPU	projectedbse	16	0.65	$9.86 \cdot 10^{-5}$	$3.63 \cdot 10^{-6}$
Crl ₃ small	CPU	non-Hermitian	15	2.00	$2.69 \cdot 10^{-5}$	$9.20 \cdot 10^{-1}$
Crl ₃ large	CPU	shao	48	394	$7.94 \cdot 10^{-5}$	$3.76 \cdot 10^{-6}$
Crl ₃ large	CPU	gruning	50	416	$1.93 \cdot 10^{-5}$	$4.93 \cdot 10^{-6}$
Crl ₃ large	CPU	projectedbse	51	403	$7.88 \cdot 10^{-5}$	$7.61 \cdot 10^{-6}$
Crl ₃ large	CPU	non-Hermitian	47	876	$6.54 \cdot 10^{-5}$	$7.79 \cdot 10^{-1}$
pentadiag small	GPU	shao	152	5.84	$2.60 \cdot 10^{-9}$	$1.55 \cdot 10^{-14}$
pentadiag small	GPU	gruning	151	6.96	$5.00 \cdot 10^{-9}$	$2.73 \cdot 10^{-10}$
pentadiag small	GPU	projectedbse	152	9.00	$2.60 \cdot 10^{-9}$	$1.50 \cdot 10^{-14}$
pentadiag small	GPU	non-Hermitian	150	15.99	$9.71 \cdot 10^{-9}$	$5.60 \cdot 10^{-6}$
pentadiag large	GPU	shao	6628	579	$2.65 \cdot 10^{-9}$	$1.11 \cdot 10^{-13}$
pentadiag large	GPU	gruning	6483	625	$5.56 \cdot 10^{-9}$	$6.16 \cdot 10^{-10}$
pentadiag large	GPU	projectedbse	6572	717	$2.61 \cdot 10^{-9}$	$1.15 \cdot 10^{-13}$
pentadiag large	GPU	non-Hermitian	3280	542	$9.57 \cdot 10^{-9}$	$4.84 \cdot 10^{-2}$
Crl ₃ small	GPU	shao	16	0.69	$9.70 \cdot 10^{-5}$	$2.03 \cdot 10^{-6}$
Crl ₃ small	GPU	gruning	17	0.86	$5.65 \cdot 10^{-6}$	$3.13 \cdot 10^{-6}$
Crl ₃ small	GPU	projectedbse	15	0.92	$1.01 \cdot 10^{-4}$	$4.30 \cdot 10^{-6}$
Crl ₃ small	GPU	non-Hermitian	21	2.14	$2.73 \cdot 10^{-5}$	$9.53 \cdot 10^{-1}$
Crl ₃ large	GPU	shao	50	9.23	$8.39 \cdot 10^{-5}$	$6.51 \cdot 10^{-6}$
Crl ₃ large	GPU	gruning	50	10.33	$1.15 \cdot 10^{-5}$	$6.33 \cdot 10^{-6}$
Crl ₃ large	GPU	projectedbse	51	10.73	$8.20 \cdot 10^{-5}$	$6.53 \cdot 10^{-6}$
Crl ₃ large	GPU	non-Hermitian	92	30.94	$8.84 \cdot 10^{-5}$	$5.27 \cdot 10^{-1}$

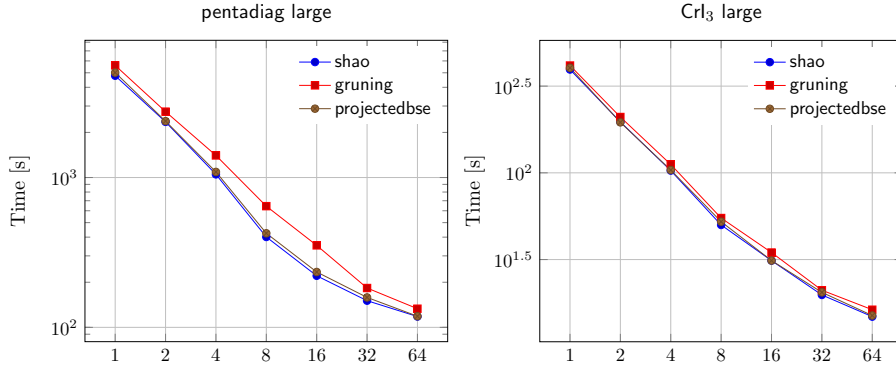


Figure 2: Parallel execution time on CPU for the **pentadiag large** test on the left, and **Crl₃ large** test on the right, for an increasing number of MPI processes.

maybe because the size of the subspace (**ncv**) is larger. Still, the execution time of the non-Hermitian solver is in general significantly larger than that of the structured solvers. Among the structured solvers, **gruning** is slightly slower than the other two in CPU, probably due to having to read a second vector basis from memory. When running on GPU, it is **projectedbse** that needs more time, which indicates some inefficiencies probably related to synchronizing data between the GPU and CPU memory.

In terms of accuracy, all solutions computed by all solvers have a relative residual smaller than the tolerance in double precision calculations, while in single precision the residual is slightly larger than the tolerance in some cases. Table 2 shows the maximum relative residual of all computed eigentriplets $(\tilde{\lambda}_i, \tilde{x}_i, \tilde{y}_i)$, $i = 1, \dots, \mathbf{nev}$, evaluated as

$$\max\{\|H\tilde{x}_i - \tilde{\lambda}_i\tilde{x}_i\|_2, \|\tilde{y}_i^*H - \tilde{y}_i^*\tilde{\lambda}_i\|_2\}/|\tilde{\lambda}_i|. \quad (26)$$

Remember that eigenvectors are normalized such that $\|\tilde{x}_i\|_2 = 1$ and $\|\tilde{y}_i\|_2 = 1$. The table also shows a quantification of the bi-orthogonality of computed eigenvectors, evaluated as $\|\tilde{Y}^*\tilde{X} - \Delta\|_{\max}$, where $\Delta = \text{diag}(\tilde{y}_i^*\tilde{x}_i)$. We can see that the structured eigensolvers enforce bi-orthogonality up to the prescribed tolerance, while eigenvectors computed by the non-Hermitian solver fail to satisfy this property, as expected. Another comment is that the structured eigensolvers return real eigenvalues, while in the case of the non-Hermitian solver the eigenvalues will have an imaginary part that can be as large as $1.4 \cdot 10^{-10}$ in **pentadiag** and $1.4 \cdot 10^{-7}$ in **Crl₃**.

Finally, we evaluate the parallel scalability of the new solvers. Section 5 plots execution times on CPU of the new eigensolvers for the two large test cases when increasing the number of MPI processes. As expected, scalability is a bit worse in the case of dense matrices. A more comprehensive performance study with Yambo matrices up to size 103680 can be found in [25].

6 Concluding remarks

We have developed three new Lanczos-type eigensolvers for the Bethe–Salpeter eigenvalue problem. The methods rely on previously proposed structure-preserving Lanczos recurrences, but we have incorporated all the details required for a robust and efficient practical implementation. In particular, all the details related to thick restart and reorthogonalization have been worked out. The result is production-quality solvers, incorporated in the SLEPc library, that can be readily used by applications such as Yambo. According to [25], the performance of the eigenvalue solution in Yambo simulations has improved in an order of magnitude, compared to the previous solution approach (two-sided non-Hermitian Krylov-Schur with the same value of the **ncv**

parameter). This will enable Yambo users to perform more detailed analyses involving larger matrices with a more effective use of supercomputer allocated time. The results in section 5 also show that the computed solution is more accurate.

In this paper we have assumed that the number of wanted eigenvalues is in the order of hundreds or less. However, some of the application articles using the Yambo code that were cited in section 1 compute a few thousand eigenvalues. In that case, the performance of our solvers will likely degrade due to the increased cost of full orthogonalization. An alternative would be to use some kind of semi-orthogonalization, but the robustness of this approach might be compromised when combined with thick restart. As an ongoing effort, we are considering spectrum slicing strategies, where eigenvalues are computed in chunks. In particular, we are working out the details of a polynomial filtering method adapted to the Bethe–Salpeter matrix.

Acknowledgements We would like to thank Davide Sangalli for providing us with the Yambo test matrices used in section 5, and for fruitful discussion and interaction that led to improvements in the interface between Yambo and SLEPc.

References

- [1] F. Alvarruiz, C. Campos, and J. E. Roman. Thick-restarted joint Lanczos bidiagonalization for the GSVD. *J. Comput. Appl. Math.*, 440:115506, 2024.
- [2] C. Attaccalite, M. Grüning, and A. Marini. Real-time approach to the optical properties of solids and nanostructures: Time-dependent Bethe-Salpeter equation. *Phys. Rev. B*, 84(24), 2011.
- [3] Z. Bai and R.-C. Li. Minimization principles for the linear response eigenvalue problem I: Theory. *SIAM J. Matrix Anal. Appl.*, 33(4):1075–1100, 2012.
- [4] Z. Bai and R.-C. Li. Minimization principles for the linear response eigenvalue problem II: Computation. *SIAM J. Matrix Anal. Appl.*, 34(2):392–416, 2013.
- [5] P. Benner, H. Faßbender, and M. Stoll. Solving large-scale quadratic eigenvalue problems with Hamiltonian eigenstructure using a structure-preserving Krylov subspace method. *Electron. Trans. Numer. Anal.*, 29:212–229, 2008.
- [6] P. Benner, H. Faßbender, and M. Stoll. A Hamiltonian Krylov–Schur-type method based on the symplectic Lanczos process. *Linear Algebra Appl.*, 435(3):578–600, 2011.
- [7] P. Benner, H. Faßbender, and C. Yang. Some remarks on the complex J-symmetric eigenproblem. *Linear Algebra Appl.*, 544:407–442, 2018.
- [8] P. Benner and C. Penke. Efficient and accurate algorithms for solving the Bethe–Salpeter eigenvalue problem for crystalline systems. *J. Comput. Appl. Math.*, 400:113650, 2022.
- [9] F. Bruneval, T. Rangel, S. M. Hamed, M. Shao, C. Yang, and J. B. Neaton. MOLGW 1: Many-body perturbation theory software for atoms, molecules, and clusters. *Comput. Phys. Commun.*, 208:149–161, 2016.
- [10] A. Bunse-Gerstner, R. Byers, and V. Mehrmann. A chart of numerical methods for structured eigenvalue problems. *SIAM J. Matrix Anal. Appl.*, 13(2):419–453, 1992.
- [11] C. Campos and J. E. Roman. Restarted Q-Arnoldi-type methods exploiting symmetry in quadratic eigenvalue problems. *BIT*, 56(4):1213–1236, 2016.

- [12] J. Cervantes-Villanueva, F. Paleari, A. García-Cristóbal, D. Sangalli, and A. Molina-Sánchez. Excitons in layered BiI_3 : Effects of dimensionality and crystal anisotropy. *Phys. Rev. B*, 109(15), 2024.
- [13] J. Deslippe, G. Samsonidze, D. A. Strubbe, M. Jain, M. L. Cohen, and S. G. Louie. BerkeleyGW: A massively parallel computer package for the calculation of the quasiparticle and optical properties of materials and nanostructures. *Comput. Phys. Commun.*, 183(6):1269–1289, 2012.
- [14] H. Fassbender and D. Kressner. Structured eigenvalue problems. *GAMM Mitt.*, 29(2):297–318, 2006.
- [15] M. Grüning, A. Marini, and X. Gonze. Implementation and testing of Lanczos-based algorithms for Random-Phase Approximation eigenproblems. *Comput. Mater. Sci.*, 50(7):2148–2156, 2011.
- [16] R. Haydock. The recursive solution of the Schrödinger equation. In H. Ehrenreich, F. Seitz, and D. Turnbull, editors, *Solid State Physics*, volume 35, pages 215–294. Academic Press, 1980.
- [17] V. Hernandez, J. E. Roman, and A. Tomas. Parallel Arnoldi eigensolvers with enhanced scalability via global communications rearrangement. *Parallel Comput.*, 33(7–8):521–540, 2007.
- [18] V. Hernandez, J. E. Roman, and A. Tomas. A robust and efficient parallel SVD solver based on restarted Lanczos bidiagonalization. *Electron. Trans. Numer. Anal.*, 31:68–85, 2008.
- [19] V. Hernandez, J. E. Roman, and V. Vidal. SLEPc: A scalable and flexible toolkit for the solution of eigenvalue problems. *ACM Trans. Math. Software*, 31(3):351–362, 2005.
- [20] Z. Kandemir, P. D’Amico, G. Sesti, C. Cardoso, M. V. Milošević, and C. Sevik. Optical properties of metallic MXene multilayers through advanced first-principles calculations. *Phys. Rev. Mater.*, 8(7), 2024.
- [21] D. Kressner. *Numerical Methods for General and Structured Eigenvalue Problems*, volume 46 of *Lecture Notes in Computational Science and Engineering*. Springer, Berlin, 2005.
- [22] D. Kressner. A periodic Krylov-Schur algorithm for large matrix products. *Numer. Math.*, 103(3):461–483, 2006.
- [23] A. Marini, C. Hogan, M. Grüning, and D. Varsano. yambo: An ab initio tool for excited state calculations. *Comput. Phys. Commun.*, 180(8):1392–1403, 2009.
- [24] V. Mehrmann and D. Watkins. Structure-preserving methods for computing eigenpairs of large sparse skew-Hamiltonian/Hamiltonian pencils. *SIAM J. Sci. Comput.*, 22(6):1905–1925, 2001.
- [25] P. Milev, B. Mellado-Pinto, M. Nalabothula, A. Esquembre-Kučukalić, F. Alvarruiz, E. Ramos, L. Wirtz, J. E. Roman, and D. Sangalli. Performances in solving the Bethe–Salpeter equation with the Yambo code. Preprint submitted to Euro-Par conference, 2025.

- [26] C. Penke. *Efficient algorithms for solving structured eigenvalue problems arising in the description of electronic excitations*. PhD thesis, Otto-von-Guericke Universität, Magdeburg, 2022.
- [27] C. Penke, A. Marek, C. Vorwerk, C. Draxl, and P. Benner. High performance solution of skew-symmetric eigenvalue problems with applications in solving the Bethe-Salpeter eigenvalue problem. *Parallel Comput.*, 96:102639, 2020.
- [28] E. E. Salpeter and H. A. Bethe. A relativistic equation for bound-state problems. *Phys. Rev.*, 84(6):1232–1242, 1951.
- [29] D. Sangalli, A. Ferretti, H. Miranda, C. Attaccalite, I. Marri, E. Cannuccia, P. Melo, M. Marsili, F. Paleari, A. Marrazzo, G. Prandini, P. Bonfà, M. O. Atambo, F. Affinito, M. Palummo, A. Molina-Sánchez, C. Hogan, M. Grüning, D. Varsano, and A. Marini. Many-body perturbation theory calculations using the yambo code. *J. Condens. Matter Phys.*, 31(32):325902, 2019.
- [30] M. Shao, F. H. da Jornada, L. Lin, C. Yang, J. Deslippe, and S. G. Louie. A structure preserving Lanczos algorithm for computing the optical absorption spectrum. *SIAM J. Matrix Anal. Appl.*, 39(2):683–711, 2018.
- [31] M. Shao, F. H. da Jornada, C. Yang, J. Deslippe, and S. G. Louie. Structure preserving parallel algorithms for solving the Bethe–Salpeter eigenvalue problem. *Linear Algebra Appl.*, 488:148–167, 2016.
- [32] Horst D. Simon and Hongyuan Zha. Low-rank matrix approximation using the Lanczos bidiagonalization process with applications. *SIAM J. Sci. Comput.*, 21(6):2257–2274, 2000.
- [33] G. W. Stewart. A Krylov–Schur algorithm for large eigenproblems. *SIAM J. Matrix Anal. Appl.*, 23(3):601–614, 2001.
- [34] D. M. N. Thomen, C. Sevik, M. V. Milošević, L. K. Teles, and A. Chaves. Strain and stacking registry effects on the hyperbolicity of exciton polaritons in few-layer black phosphorus. *Phys. Rev. B*, 109(24), 2024.
- [35] G. Tirimbò, V. Sundaram, O. Çaylak, W. Scharpach, J. Sijen, C. Junghans, J. Brown, F. Zapata Ruiz, N. Renaud, J. Wehner, and B. Baumeier. Excited-state electronic structure of molecules using many-body Green’s functions: Quasiparticles and electron–hole excitations with VOTCA-XTP. *J. Chem. Phys.*, 152(11), 2020.
- [36] D. S. Watkins. On Hamiltonian and symplectic Lanczos processes. *Linear Algebra Appl.*, 385:23–45, 2004.
- [37] K. Wu and H. Simon. Thick-restart Lanczos method for large symmetric eigenvalue problems. *SIAM J. Matrix Anal. Appl.*, 22(2):602–616, 2000.
- [38] T. Zhang and F. Xue. A Chebyshev locally optimal block preconditioned conjugate gradient method for product and standard symmetric eigenvalue problems. *SIAM J. Matrix Anal. Appl.*, 45(4):2211–2242, 2024.
- [39] I. N. Zwaan and M. E. Hochstenbach. Krylov–Schur-type restarts for the two-sided Arnoldi method. *SIAM J. Matrix Anal. Appl.*, 38(2):297–321, 2017.